ISSN 1063-7737, Astronomy Letters, 2008, Vol. 34, No. 7, pp. 486–499. © Pleiades Publishing, Inc., 2008.
Original Russian Text © G.P. Chernov, 2008, published in Pis'ma v Astronomicheskiĭ Zhurnal, 2008, Vol. 34, No. 7, pp. 536–550.

Unusual Stripes in Emission and Absorption in Solar Radio Bursts: Ropes of Fibers in the Meter Wave Band

G. P. Chernov*

Pushkov Institute of Terrestrial Magnetism, Ionosphere, and Radiowave Propagation (IZMIRAN), Russian Academy of Sciences, Troitsk, Moscow oblast, 142190 Russia

Received April 26, 2007

Abstract—Based on data from the spectrographs of IZMIRAN and Tremsdorf station (Astronomical Institute, Potsdam), we analyze the ropes of narrow-band fibers in the spectra of solar radio bursts in the meter wave band by invoking events of satellite data (SOHO/LASCO, EIT, MDI) for the analysis. We consider in detail basic properties of the ropes in four events in comparison with previously known data. The fibers in ropes are more commonly observed with an overlap in time and frequency, but occasionally (more often at the end of the ropes) they can follow with a separation in time. The fiber duration and recurrence period seldom remain stable and, in general, increase from 0.3–0.5 s at the beginning to several seconds at the end of the rope. The relative values of the instantaneous and total fiber frequency bandwidths change only slightly in different events; $\delta f/f \approx 0.003$–0.005 and $\Delta f/f \approx 0.02$–0.03. Most of the ropes exhibit a low-frequency absorption. The fibers in ropes are similar to ordinary intermediate drift bursts (fiber bursts), but they drift in a narrow frequency band and have a more frequent recurrence in some events. The ropes of fibers are usually observed in the time interval when the shock front catches up with the leading edge of a coronal mass ejection. Under the condition of a unified approach to interpreting the ropes of fibers in all events, their basic properties can be explained in terms of the model of fiber bursts. The connection of fibers with the developed zebra pattern is shown within the framework of a unified approach to the formation theory of stripes in emission and absorption in the model on whistlers.

PACS numbers : 96.60.Hv; 96.60.ph
DOI: 10.1134/S1063773708070074

Key words: *Sun, radio bursts, flares, fibers, plasma waves, whistlers.*

INTRODUCTION

The stripes in emission and absorption in the form of a regular zebra pattern (ZP) or intermediate drift bursts (IDBs or fiber bursts) against the continuum background of metric and decimetric type IV radio bursts have long been studied and classified in monographs (Kruger 1979) and reviews (Slottje 1981; Chernov 2006). The ropes of narrow-band fibers, whose nature still remains poorly studied, are a variety of such structures. They were interpreted in terms of four different models that occasionally were even unrelated to the IDB and ZP models. They were first detected with the IZMIRAN spectrograph in the April 24, 1985 event and discussed by Aurass et al. (1987) (where they were called *slowly drifting chains of narrow-band fibers*) and Mann et al. (1989) (where they were called packets of fibers). Basic properties of such ropes are presented in Fig. 1: a narrow-band rope (2–3 MHz in width) generally has an arbitrarily oscillating frequency drift and consists of periodic fibers that usually drift to low frequencies and have absorptions from the low-frequency (LF) edge, which are occasionally more pronounced than the fibers in emission (see the profile under the spectrum in Fig. 1); narrow fibers usually follow with a frequency overlap and their recurrence rate is a factor of 2–3 higher than that of ordinary IDBs (Chernov 1997). Since these periodic fibers in the dynamic spectrum are actually similar in general appearance to a rope, here we will use this term. In contrast to the terms mentioned above, it does not simultaneously imply a model of their formation.

Initially, the ropes seemed to be rare events observed at the post-maximum phase of large flares and accompanying the developed ZP. However, a more careful examination of both old and new events showed that the ropes of fibers often appear in a wide frequency range of the meter wave band not only as part of the developed ZP, but also as single bursts at the impulsive phase after type III bursts and before a type II burst or even without the latter. The param-

*E-mail: gchernov@izmiran.rssi.ru

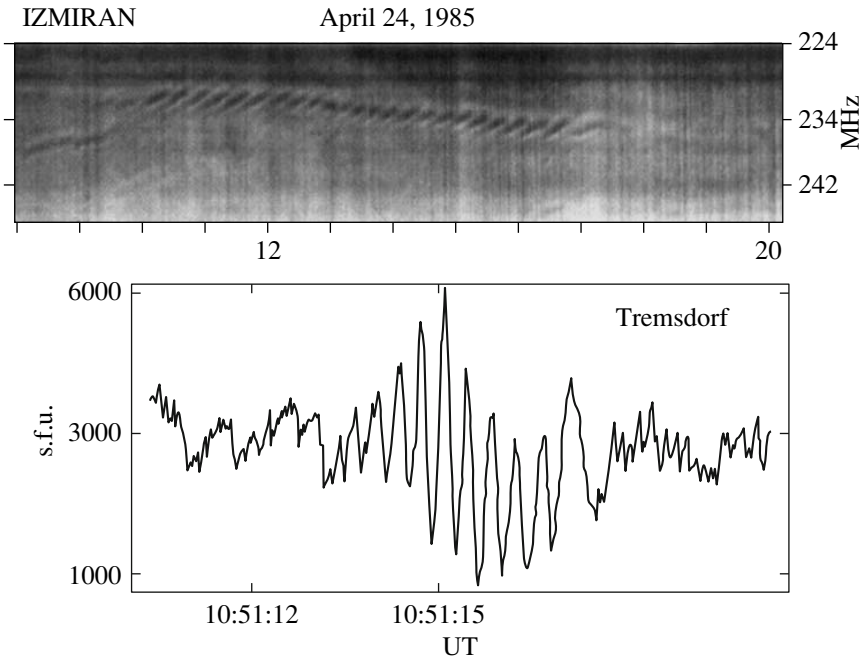

Fig. 1. Dynamic spectrum of a rope of narrow-band fibers in the April 24, 1985 event. The time profile of the intensity at 234 MHz is shown below on the same scale with the spectrum (Tremsdorf station, Potsdam).

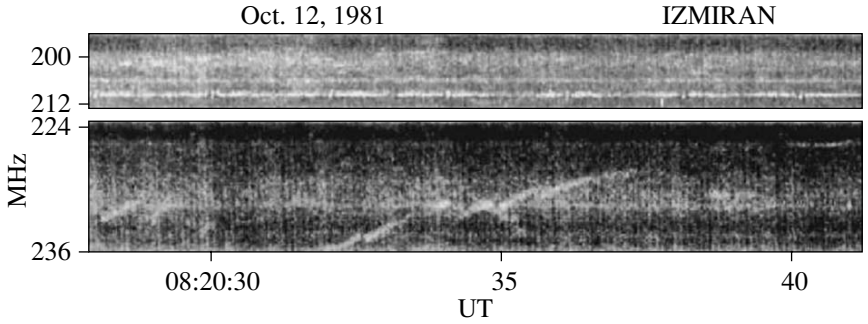

Fig. 2. Dynamic spectrum of the ropes of fibers in the large radio burst on October 12, 1981.

eters of the narrow fibers change noticeably. Thus, for example, in the large radio burst with a ZP on October 12, 1981, discussed in various aspects by Aurass and Chernov (1983) and Chernov (1997), the ropes were observed about 1 h after the ZP in the form of single bursts. We see from such a rope shown in Fig. 2 that the narrow fibers do not follow strictly periodically, with an overlap in frequency, and exhibit no absorptions from the LF edge.

Even stranger ropes were observed at lower frequencies. The analysis of the ropes of fibers in the May 2, 1998 event at 20–40 MHz performed by Chernov (2004) and in more detail by Chernov et al. (2007a) showed that narrow expanding ropes of strictly periodic fibers with a weak LF absorption were observed between two type II bursts and their radio emission should have originated from the range of heights between two shock fronts propagating with different velocities. Various ropes of fibers without any noticeable LF absorption were observed at 19–29 MHz as a fine structure of complex type II bursts (Chernov et al. 2007b). Since such ropes appeared in two events at the time when the shock wave was catching up with a coronal mass ejection (CME), the radio emission originated from the region between the leading edge of the CME and the shock front trailing behind.

One of the models suggested to explain the origin of the first ropes in the April 24, 1985 event also assumes that the radio source is located between the shock fronts emanating from the X point of magnetic reconnection high in the corona (Chernov 1997). Previously, however, they were associated with the threshold switch-on of the loss-cone

instability of whistlers when a critical loss-cone angle is exceeded due to an additional perturbation of the magnetic trap by a fast magnetosonic (FMS) wave (Mann et al. 1989). Subsequently, however, Klassen et al. (2001) and Karlicky et al. (2002) suggested a new name for one of the ropes in the November 3, 1997 event, *sawtooth* bursts, and considered new models that assumed the absence of an overlap in the spectra of individual fibers in the rope. Since other ropes with an ordinary overlap of fibers in time were observed in this event at neighboring frequencies, constructing a new model for the "sawtooth" ropes seems unjustified and this event should be analyzed in more detail in comparison with previously known and new events. It is desirable to compare the two events (on November 3, 1997, and May 6, 1998) shown in Klassen et al. (2001) with the new interesting bursts with ropes of fibers obtained at IZMIRAN on July 18, 2000, and November 8, 2004, using all of the accompanying data on flares. Such an analysis is the goal of this paper.

OBSERVATIONS

The November 3, 1997 Event

The large radio burst began with a group of type III bursts followed by type II + IV bursts during a 1B M1.4 flare in the interval 09:07–09:25 UT in the active region (AR) 8100 (S18W19). A general spectrum of the radio burst in the frequency range 40–800 MHz is shown in Klassen et al. (2001), Karlicky et al. (2002), and Khan and Aurass (2002). The large type II burst had a harmonic structure (the fundamental harmonic began approximately at 09:09 UT), while data from the spectropolarimeter of the Nancay Observatory in the frequency range 20–70 MHz suggest that each harmonic was split into 3–4 stripes drifting up to a frequency of 20 MHz. The frequency drift rate of the fundamental harmonic at 70 MHz was -0.29 MHz s^{-1}. This corresponds to a shock velocity of $\sim$1540 km s^{-1} in the doubled Newkirk density model in the corona.

Subsequently, however, the burst had no continuation in the WIND/WAVE spectrum (below 14 MHz). The type III bursts were a direct continuation of the rapidly drifting bursts from the centimeter range (according to the spectra of the Ondrejov Observatory spectrograph in the frequency range 1–4.5 GHz), pointing to the location of particle acceleration directly in the flare region. Therefore, we provide here only additional data—the simultaneous IZMIRAN and Potsdam (Tremsdorf station) dynamic spectra of the ropes of fibers (Fig. 3).

Parameters of the Ropes of Fibers

We see from Fig. 3 that the appearance of the rope of fibers in the interval 09:09–09:10 UT at frequencies near 150 MHz coincided with the onset of the type II burst; this can be traced more clearly by the stripe of the second harmonic drifting from frequencies of $\sim$350 MHz in the upper Tremsdorf spectrum. However, during the previous minute (09:08–09:09), we can see (better in the IZMIRAN spectrum) two more ropes, one also around 150 MHz and the other at 210–215 MHz. In both ropes, the fibers followed with an appreciable overlap in time. In the last rope, the fiber recurrence rate was much higher (a period of $\sim$1 s), although the fibers in the first rope did not follow strictly periodically, while in the strongest rope (09:09–09:10 UT) the period gradually increased from about 4.5 s in the first three fibers to 8 s in the subsequent four fibers. This is clearly shown in Fig. 4, in which the magnified fragments of this rope are presented on the same time scale in the IZMIRAN and Tremsdord spectra. Note that all features of the fibers closely coincide at both observatories, which confirms the solar (rather than ionospheric) origin of such structures. It is important to note that the increasing period pertains to the main fibers in the rope. However, shorter fragments similar to the partial frequency splitting of the main fibers by $\sim$1.5 MHz appear between them at the ends of the first five fibers.

The fiber duration (Δt) was not constant. It increased from the first fiber to the sixth one from 4–5 s to $\sim$9 s, although it reached 18 s in the first rope at 150 MHz and was shortest, 3–4 s, at 210–215 MHz. In the two preceding ropes, no clear gradual increase in fiber duration was observed. The overlap of the fibers in time and frequency was largest in the rope at 215 MHz; three fibers overlapped simultaneously. There is no harmonic connection between the fibers.

There is virtually no frequency drift of the first two ropes, while the brightest rope at 09:09–09:10 had a frequency drift rate $df/dt \sim -0.17$ MHz s^{-1} that was almost a factor of 2 smaller than that for the fundamental tone of the type II burst. The frequency drift rate of the individual fibers was stable, -0.38 MHz s^{-1}, which is approximately equal to the drift rate of the fundamental tone of the type II burst at the same frequencies. In the first rope, the fiber drift rate was approximately the same or lower (it was not stable). In the rope at 210–215 MHz, the fiber drift rate is approximately equal to that of the second harmonic of the type II burst, ~ -0.70 MHz s^{-1}.

The width of the frequency band (Δf) occupied by an individual fiber was 3–4 MHz at maximum. The instantaneous frequency bandwidth of an individual fiber was $\delta f \approx 0.5$–0.75 MHz at 150 MHz, i.e., the

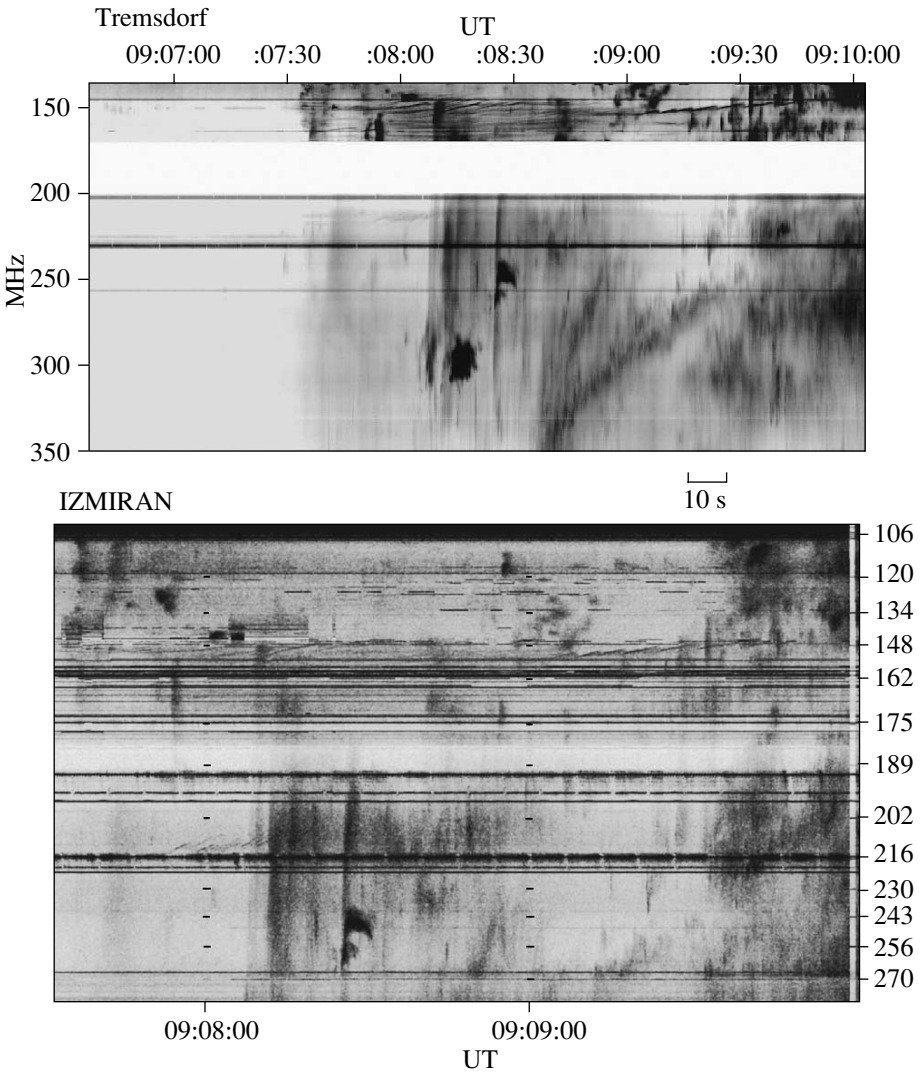

Fig. 3. Comparison of the fragments of the Tremsdorf (Potsdam) and IZMIRAN spectra at the beginning of the November 3, 1997 event on different time and frequency scales.

maximum relative bandwidth was $\delta f/f \approx 0.005$. A small absorption from the LF edge can be noticed in the main bright rope (we see from Fig. 4 that the fibers in the rope are the noticeable LF boundary of the flare continuum). In the other two ropes, the absorption, if any, is near the detection threshold.

Thus, three ropes of fibers with different parameters appeared during two minutes. The fibers in the ropes are similar in several parameters to intermediate drift bursts, differing only by the lower frequency drift rate (approximately by a factor of 2) and the narrower frequency band in the spectrum Δf. Each rope was accompanied by several type III bursts, but there was no correspondence between the individual fibers in the rope and the periodic type III bursts. It can be said with confidence that the rope at 09:09–09:10 was accompanied by a herringbone structure originating from the LF edge of the fundamental tone of the type II burst (Fig. 4). Several similar ropes were also observed with the Nancay spectropolarimeter in the same time interval at 50–25 MHz. The only difference between the ropes in the Nancay spectra is their more chaotic appearance, the absence of a strict periodicity. The polarization of the radio emission both from the entire type II burst and from the ropes was weak (<10%) and left-handed.

Description of Accompanying Events

The presence of several U bursts suggests that there are closed magnetic loops in the corona at the heights of plasma levels 240–260 MHz into which some of the particles responsible for the type III bursts were trapped. According to the *Solar Geophysical*

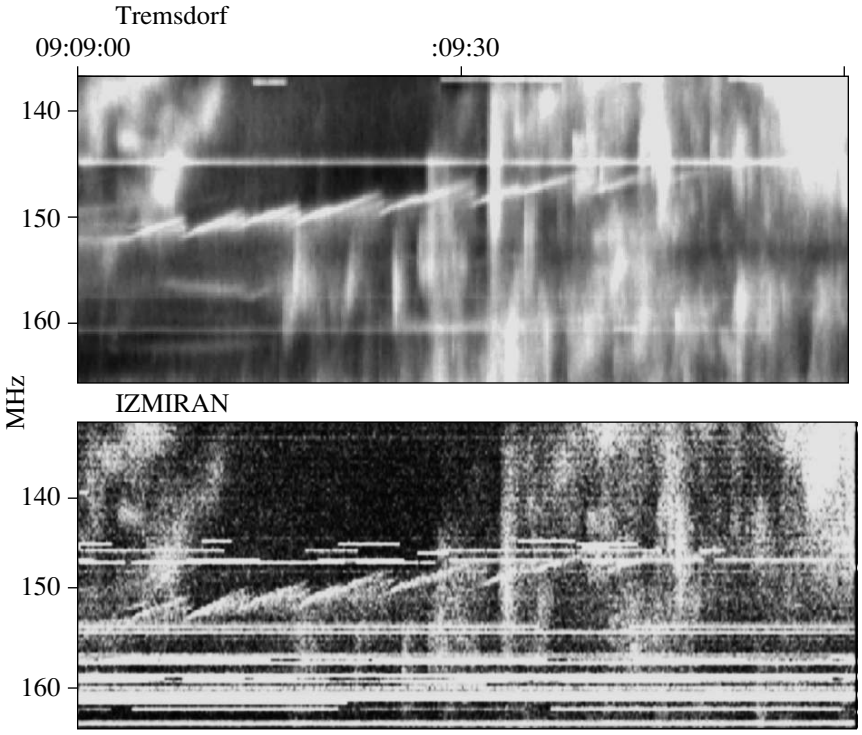

Fig. 4. Magnified fragments of the Tremsdorf and IZMIRAN spectra (on the same time scale) showing a close coincidence between the rope of fibers and all of the accompanying bursts in the November 3, 1997 event.

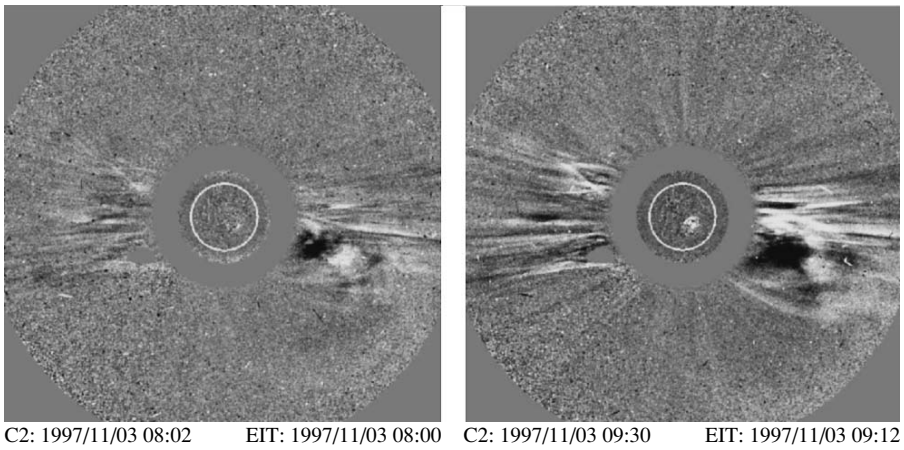

Fig. 5. Two differential images from the SOHO/LASCO C2 video clip for November 3, 1997: the onset of CME at 09:30 (right panel) occurred against the background of the perturbations left from the preceding CME (left panel).

Data, the peak radio flux was recorded in the meter wave band, 23 000 s.f.u. at 245 MHz (1 s.f.u. = 10^{-22} W m^{-2} Hz^{-1}).

The event was accompanied by a slow CME; the first frame from the video clip of differential images for this ejection at 09:30 UT is shown on the right panel of Fig. 5. It is important to note that this ejection propagated in the tail of the preceding CME whose track is shown on the left panel of Fig. 5. It demonstrates the residual moving coronal inhomogeneities (light narrow and clumpy structures). Figure 6 shows the height–time diagram with three reliable CME positions marked by the asterisks through which the fitting straight line was drawn to the center of the Sun. The crosses mark the shock front positions calculated (within the framework of the doubled Newkirk density model) from the dynamic spectrum of the type II burst. The corresponding frequencies are indicated to the right of the crosses. The shock front velocity was approximately a factor of 4.5 higher and

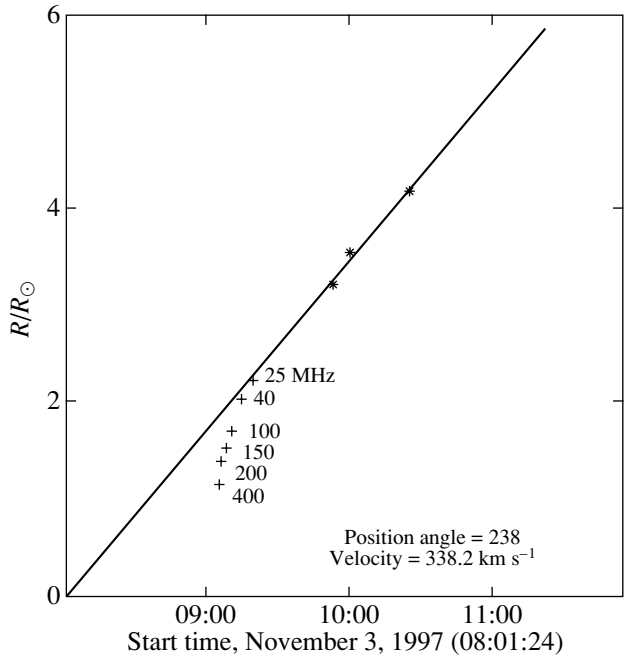

Fig. 6. Height–time diagram for CME at 09:30 (SOHO/LASCO catalog). The crosses mark the positions of the shock front and the corresponding frequencies calculated (within the framework of the doubled Newkirk density model) from the dynamic spectrum of the type II burst; the shock front caught up with CME approximately at 09:25 UT.

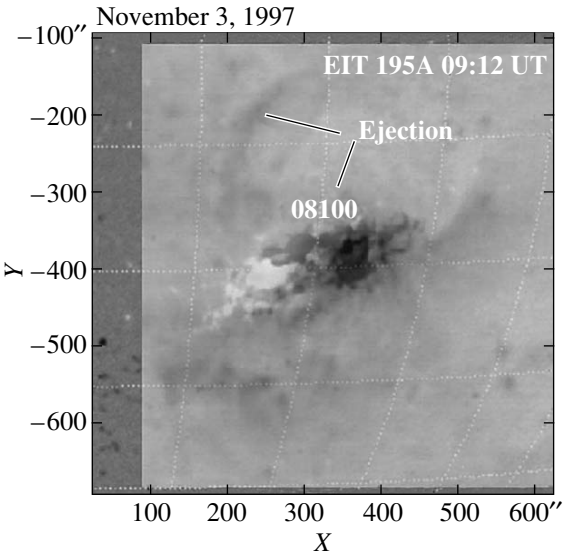

Fig. 7. Semitransparent superposition of the (SOHO/EIT) flare image in the 195 Å line on the (SOHO/MDI) magnetogram of AR 08100. The brightest (black in the image) part of the flare was located above the leading sunspot. An oval ejection (Moreton wave) diverges symmetrically from it; the remnants of the direct ejection inclined to the NE direction are also seen.

the shock front caught up with the fitted disturbance approximately at 09:25 (the time of intersection with the straight line).

The type II burst stopped at 20 MHz exactly at this time and had no continuation at lower frequencies. Upon its interaction with a magnetic cloud (CME), the shock front ceased to exist (or was transformed into a slow shock front). It thus follows that our ropes appeared in the interval 09:08–09:10, when the shock front was approaching the lower edge of the CME while propagating in its wake. We have no information about the CME generation height, but the maximum energy release at the heights of the meter wave band (245 MHz) and the large number of U bursts in the range 200–260 MHz are indicative of the possible beginning of the ejection at these heights. Note that the dark filament in the Hα line located on the western outskirts of AR 8100 disappeared on the next day. Although the time of its disappearance is unknown, the very disappearance of the filament supports the assumption about an initial CME height of ~100–150 thousand km.

The shock front generation can be traced in Fig. 7, in which the (SOHO/EIT) flare image in the extreme ultraviolet 195 Å line at 09:12 (close to the maximum in soft X rays) is superimposed on the SOHO/MDI magnetogram. Two effects can be distinguished: the brightest part of the flare (black against the gray background) was located above the leading sunspot of southern magnetic polarity (the maximum in soft X rays was also located there); two ejections marked by the arrows emanate from this region. The propagating oval front can be associated with the appearance of the type II burst, which is known to appear only at the heights of the Alfvén velocity minimum (in the meter wave band). A similar conclusion was reached by Khan and Aurass (2002), who reliably showed that the Moreton wave in the Hα image coincided with the wave in the EIT 195 Å image and with the propagating front in the soft X-ray (Yohkoh/SXT) image. In addition, according to the Nancay radio heliograph data at 164, 236.6, 327, 410.5, and 432 MHz, the centers of the moving radio sources of the type II burst coincided with this front. The propagation velocity of the Moreton wave and the front in soft X rays, ~540–560 km s^{-1}, obtained by Khan and Aurass (2002) is considerably lower than our estimate of the shock front velocity (1540 km s^{-1}). This may be because the shock front propagated radially, while the Moreton wave propagated horizontally (in projection onto the photosphere). The shock front velocities obtained by Khan and Aurass (2002) (from 560 to 1100 km s^{-1} for different type II burst components) were underestimated, since they were determined in a model with an underestimated electron number den-

sity from the barometric formula derived by Mann et al. (1999), which is valid for the quiet corona. The doubled Newkirk density model we used coincides with the numerous density estimates obtained from radio data above an active region.

Thus, the meter radio emission source should be located in the range of heights between the CME and the shock front catching up with it. The latter propagated through narrow density inhomogeneities in the CME tail. The rope formation process covered the entire meter wave band very quickly. Taking into account the delay in the appearance of ropes at 50 MHz at 09:08:55 relative to 210 MHz at 09:07:45, we find the propagation velocity of the disturbance (within the framework of the doubled Newkirk density model) to be about 6400 km s^{-1}.

The high velocity of the disturbance can be easily explained when it is considered that the oval ejection continued to propagate into the corona. On the right panel of Fig. 5, we can see an advancing oblique loop that is probably an extension of the loop-shaped ejection indicated by the arrows in Fig. 7 high in the corona. The expanding oblique shock front can cover the range of heights of the meter radio source in the radial direction much faster than during the direct radial propagation, provided that the radio emission originates from the narrow radial inhomogeneities. The presence of a rich herringbone structure suggests a periodic acceleration of particles at the shock front, which were then trapped into the CME magnetic cloud, filling a wide range of heights. The type II burst appeared already against the background of the flare continuum; the ropes also formed against its background. The ropes may have been excited only upstream of the shock front (if judged from the set of events; see the July 18, 2000 event below).

Interestingly, an even more intense type II burst was observed at 10:29 UT after the November 3, 1997 under discussion, which was also accompanied by CME, but no ropes of fibers were observed at any flare phase. A similar analysis of the positions of the shock front and CME in the corona showed that, in this case, the shock front went high into the corona, higher than the initial CME heights. Therefore, there were no conditions for the trapping of particles accelerated at the shock front.

The May 6, 1998 Event

The May 6, 1998 flare was also accompanied by a similar order of type III radio bursts followed by type II and IV bursts. The maximum energy release also took place in the meter wave band: at the type II burst peak at 08:06 UT, the flux at 245 MHz was 65 000 s.f.u. The flare occurred in the same AR 8210 as the May 2, 1998 event with record ropes (Chernov et al. 2007a). However, only one rope of fibers was detected in this case. A general appearance of the dynamic spectrum is shown in the upper panel of Fig. 8. The rope also appeared before the type II burst. Magnified fragments of the IZMIRAN and Tremsdorf spectra for the rope are shown in the two lower panels of Fig. 8. Although the brightness of the IZMIRAN spectrum was reduced to record the intense event, all features of the rope and accompanying bursts closely coincide in both spectra.

The flare was accompanied by a fast CME like a partial halo with a width of 294° and a velocity of 1099 km s^{-1}. The shock front velocity determined from the brightest drifting stripes of the type II burst at 08:05:15 in Fig. 8 turned out to be considerably higher, ~2900 km s^{-1}. Comparison of the diagrams of motion for the CME and the shock front (similar to those in Fig. 6) suggests that the shock front overtook the CME in the interval 08:05–08:06, i.e., immediately after the appearance of the rope. Thus, the absence of recurrent ropes of fibers stems from the fact that there was no trap for particles upstream of the shock front after this time. The type II burst had a continuation at low frequencies in the WIND/WAVE spectrum in the range 14–5 MHz with the same peculiarity—a high frequency drift rate. The shock front can be said to have passed through the CME almost without any consequences, without acceleration, while the CME was still recorded at heights $\sim 26R_\odot$. The diffuse loop background, the probable tail from the shock front, can still be seen before the bright ejection (the leading CME edge) in the (LASCO C2) image of the CME at 08:29.

The rope parameters at frequencies near 260 MHz are $\Delta f \approx 6$ MHz and $\delta f \approx 0.8$ MHz ($\delta f/f \approx 0.003$), i.e., the relative values are approximately the same as those for the rope at 09:09–09:10 in the November 3, 1997 event. The fiber frequency drift (df/dt) was stable, ≈ -0.8 MHz s^{-1} (faster than that for the type II burst). The duration of the individual fibers changed even more chaotically, as did the period between the fibers (Fig. 8). The type III bursts also appeared during the rope, but without any unambiguous association with the fibers. The fibers initially followed with a small overlap in time, while the last two fibers followed with a noticeable gap of 3.5 s. The fibers are accompanied by a weak LF absorption, which is most pronounced at the beginning of the rope at 09:04:40 UT.

The July 18, 2000 Event

This event differs from the two previous events by the absence of a type II burst and CME. Numerous ropes of fibers were observed for three minutes in the

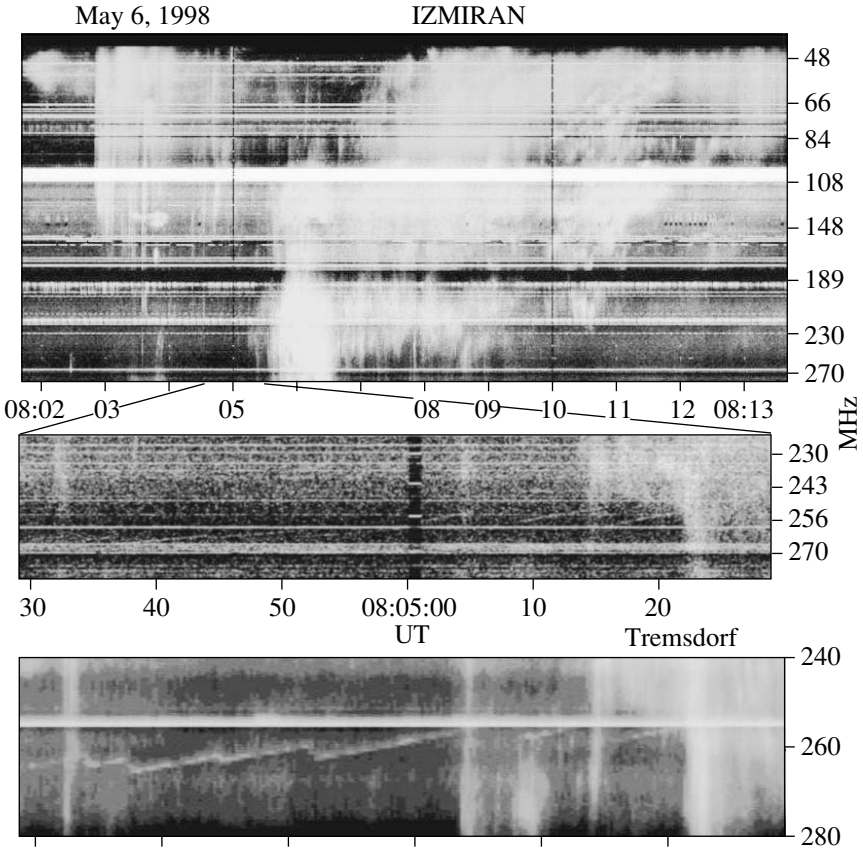

Fig. 8. IZMIRAN dynamic spectrum (45–270 MHz) for the beginning of the May 6, 1998 event (upper panel). On the two lower panels, the magnified fragments of the ropes of fibers in the IZMIRAN and Tremsdorf spectra show a close coincidence of all burst features on the same time scale.

flare continuum as part of the developed ZP after the group of strong type III + V bursts shown in the IZMIRAN spectrum in Fig. 9. The bursts are associated with a small C9.3 1F flare in AR 9087 (S13E16). However, the peak radio flux was also recorded in the meter wave band: 4400 s.f.u. at 245 MHz (54 s.f.u. at 2695 MHz).

The first groups of fibers appeared at 09:23:00 directly against the background of type III bursts at 270–275 MHz. They followed with a period of ~1 s, but narrow ropes with an overlap in time and with a period of ~0.25 s appeared several seconds later. The ZP shown on the magnified fragment of the spectrum in Fig. 9 developed in the 200–270 MHz band almost simultaneously. In addition to the largest rope with a bandwidth Δf gradually decreasing from 5 to 2 MHz and an increasing frequency drift rate, up to ten more small ropes with various frequency drift rates and with a period of the fibers in the rope of 0.25 s can be distinguished on this fragment. All ropes exhibit deep continuum absorptions from the LF edge (with a higher contrast than those in the ZP). This can be clearly judged from the intensity profiles at two frequencies shown under the spectrum on the same time scale. The largest rope of fibers and several neighboring small ropes at the beginning of the fragment turned out to be embedded in a wide absorption region whose bandwidth exceeds appreciably that of the ropes in emission. The strange wide fiber with a wavy frequency drift at the end of the fragment also stands out sharply against the ZP background by its higher-contrast absorption. This fiber can even be interpreted as an underdeveloped rope: the emission from the wide fiber had no time to break up into small fibers. Subsequently (at about 09:26), the ZP near 256 MHz exhibited zigzags similar to this fiber. More than ten additional (small and large) ropes appeared during the next minute (09:24–09:25); all of them appeared at lower frequencies together with the ZP (Fig. 10). Thus, we can talk about the high-frequency boundary of appearance of the ropes drifting toward the low frequencies at a rate typical of type II bursts. The drift of the ropes themselves became more stable (it changed only smoothly) and the following general tendency is clearly traceable: most of the ropes were aligned along this boundary. Thus, we indirectly detect a traveling disturbance, possibly, a shock wave.

The minimum fiber bandwidth δf at frequencies

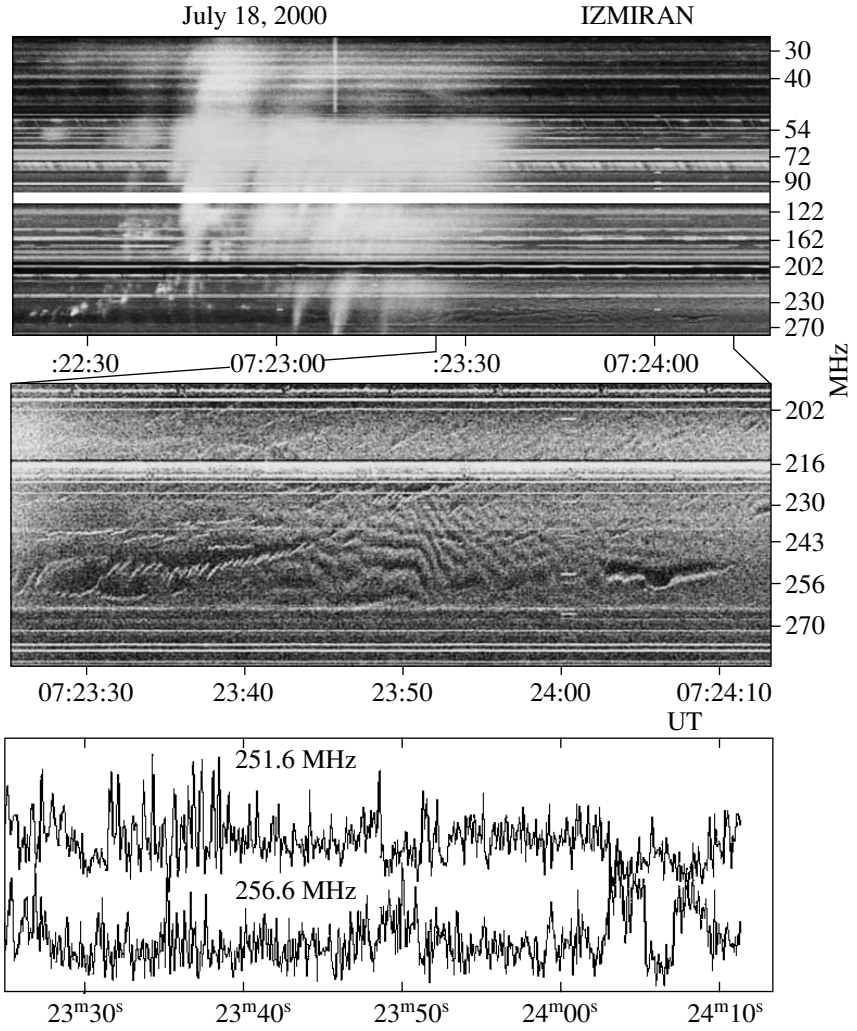

Fig. 9. IZMIRAN dynamic spectrum (25–270 MHz) for the beginning of the July 18, 2000 event (upper panel). The middle panel shows a magnified fragment of the rope of fibers in the developed ZP. The intensity profiles are shown below on the same time scale with a magnified spectrum; they show the modulation depth of the emission during the rope (251.6-MHz profile) and a single zigzag fiber (256.6-MHz profile).

near 250 MHz was about 0.76 MHz (a relative bandwidth $\delta f/f \approx 0.003$). The ropes had various durations. Wavy variations near zero are typical of the rope frequency drift, although the drift of individual fibers was more stable, ~ -6–8 MHz s^{-1}. Such a drift is typical of ordinary fibers at these frequencies. The fiber duration Δt changed arbitrarily from 0.5 to 3 s (both in the main rope and in all of the remaining ropes).

Figure 11 shows the location of the brightest part of the flare in the 195 Å line (SOHO/EIT) against the background of the (SOHO/MDI) magnetogram for AR 9087. Although the flare kernels are scattered over the entire AR, the main flare occurred above the leading sunspot, but above the magnetic neutral line. The flare in the November 3, 1997 event had approximately the same location (Fig. 7). Therefore, the flare can be assumed to have occurred in an asymmetric configuration of magnetic field lines and the magnetic field lines most likely reconnected with the external field lines along which the accelerated electron beams responsible for the type III bursts escaped. We failed to detect any propagating wave (ejection) in the 195 Å line images (with a period of 7–12 min).

The November 8, 2004 Event

This event is a purely metric radio burst, but it is considerably weaker than the previous events; its flux at 245 MHz was only 590 s.f.u. The corresponding weak soft X-ray C1.8 flare occurred during the decline of the previous larger event in AR 0696 (N08W32).

Figure 12 presents a general appearance of the radio burst in the range 28–270 MHz (upper panel).

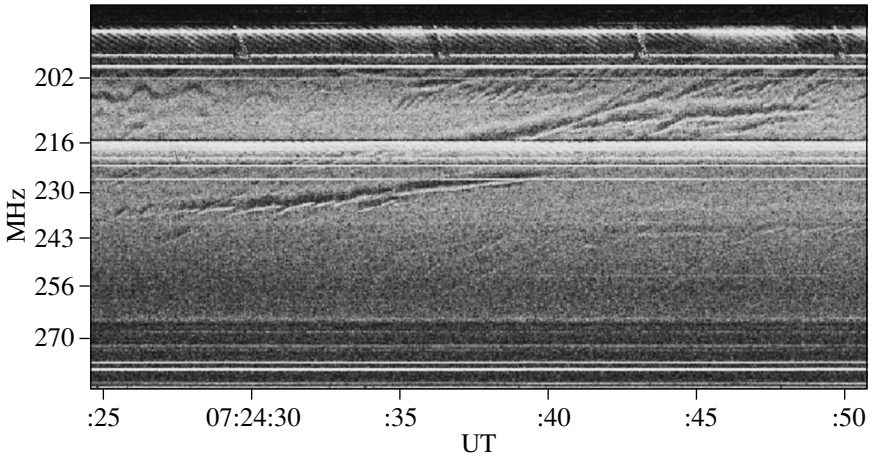

Fig. 10. Continuation of the ropes in the July 18, 2000 event in the IZMIRAN spectrum showing the high-frequency drifting boundary of appearance of the fibers; only very weak fibers (possibly those left after the shock front passage) are seen at higher frequencies.

As in all of the previous events, a complex group of type III bursts is initially observed, after which we see a chaotic group of bursts against the background of a weak flare continuum that is similar to the clumpy structure of a weak type II burst. The height–time diagram for the previous event in the SOHO/LASCO C2 catalog at 09:30 reveals an additional slow ejection (with a velocity of 213 km s^1). If the shock velocity is judged from the LF boundary of the clumps in the spectrum of Fig. 12, then it should be higher than 1000 km s^{-1}. Thus, the shock front may also have caught up with the CME in this event at a time close to the appearance of ropes of fibers.

The ropes of fibers are shown on the magnified fragment in Fig. 12. We detected a total of two ropes with different fiber periods; the second rope can be even a continuation of the first one, but with a jump in time. In addition to the ropes, we can also see several isolated fibers and a weak ZP with a positive drift of the stripes at 175–180 MHz on this fragment. The parameters of the fibers at about 160 MHz are comparable in magnitude to other events: periods $\approx$0.3–0.5 s, $\Delta t \approx 0.5$–1 s, $df/dt \approx 3$ MHz s^{-1}, and $\delta f/f \approx 0.004$. Note that the LF absorption in the ropes is very weak.

Conclusions from Observations

The ropes of fibers are formed not only in large radio bursts, but also in relatively weak ones that are not accompanied by type II bursts and CME both at the impulsive phase and at the long post-maximum phase of a flare. Comparison of the new data with previously known ones shows that all ropes of fibers are related phenomena and require a unified approach to their interpretation.

Since the ropes of fibers often appear embedded in the developed ZP, their origin is closely related to the ZP mechanism.

Analysis of the four events showed that the ropes of fibers appeared when the shock front was catching up with the CME. In the July 18, 2000 event, no CME was detected, but the type V burst and the flare continuum are indicative of a magnetic trap and magnetic reconnection high in the corona. In this

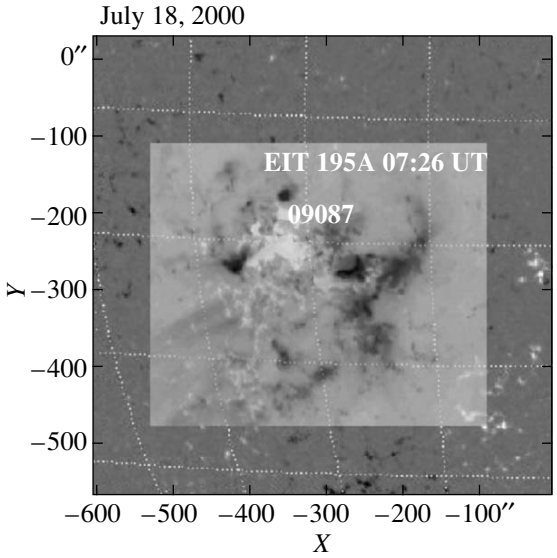

Fig. 11. Semitransparent superposition of the (SOHO/EIT) 195 Å line image of the July 18, 2000 flare on the (SOHO/MDI) magnetogram of AR 09087. The brightest (black in the image) part of the flare was located above the leading sunspot (just as for the November 3, 1997 flare).

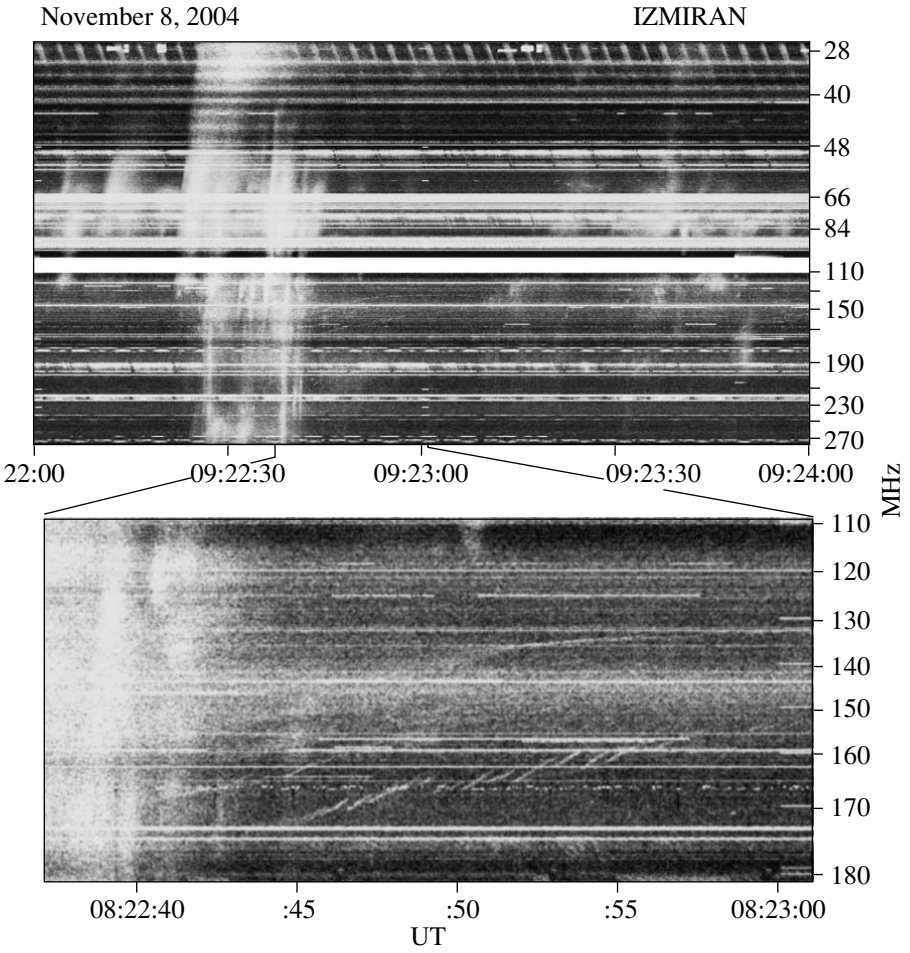

Fig. 12. IZMIRAN dynamic spectrum (25–270 MHz) for the beginning of the November 8, 2004 event (upper panel). The magnified fragment of the spectrum below shows the ropes of fibers surrounded by isolated fibers at lower frequencies and by a weak ZP at 175–180 MHz.

case, the presence of shock waves emanating from the reconnection region is also quite probable.

The rope frequency drift rate is not a governing parameter: it more often varies near zero in a wavy fashion. The frequency drift rate of the fibers in a rope is usually stable and equal to or larger than that of the type II burst.

The fibers in ropes are more commonly observed with an overlap in time and frequency, but occasionally (more often at the end of the ropes) they can follow with a gap in time. The fiber duration Δt and recurrence period seldom remain stable and, in general, increase from 0.3–0.5 s at the beginning to several seconds at the end of the rope.

The relative values of the instantaneous and total fiber frequency bandwidth change only slightly in different events: $\delta f/f \approx 0.003$–0.005 and $\Delta f/f \approx 0.02$–0.03.

Most of the ropes exhibit a LF absorption. Thus, the fibers in ropes are similar to ordinary IDBs, but they drift in a narrow frequency band and have a more frequent recurrence in some events. What is the source or formation mechanism of the ropes of fibers?

DISCUSSION

Possible Emission Mechanisms

The model of ropes in the form of a small trap between shock fronts emanating from a special X point of magnetic reconnection suggested previously (Chernov 1997) satisfies all of the conclusions from observations. The fiber generation mechanism is at work: the coalescence of plasma waves (l) with whistler wave packets (w) with the escape of an ordinary wave (t): $l + w \rightarrow t$ (Kuijpers 1975; Chernov 1976, 1990), but in a source in the form of a small ($\leqslant 10^9$ cm) magnetic trap for particles. The fiber frequency drift rate is determined by the whistler group velocity. The LF absorptions in the fibers are produced by quasi-linear effects (a reduction in the level of

plasma waves). The accompanying large fibers in absorption result from the screening of the emission from the region of rarefaction between fast and slow shock fronts in which the density is enhanced by a factor of 2–3 (see Fig. 27 from the review by Chernov (2006)). In this scheme, the variety of fiber periods and durations is associated not only with the sizes of the trap for particles and with the period of their injection, but also with the rapid damping of whistlers at the cyclotron resonance and with quasi-linear effects, which, in particular, lead to a reduction in the level of plasma waves. The Landau damping can remain insignificant (see Fig. 53 in the review by Chernov (2006)). The absence of a LF absorption means that, in this case, the particles and waves (whistlers) diverge rapidly in space.

It is well known that the plasma waves and whistlers can be excited simultaneously by the same fast particles with the loss-cone velocity distribution (Berney and Benz 1978). As applied to the solar coronal conditions, the excitation of whistlers was first considered by Kuijpers (1975). The growth rates of whistlers were calculated in more detail by Mal'tseva and Chernov (1989) by taking into account the possible peculiarities of the loss-cone distribution function. The foundations of the theory of interaction between whistlers and plasma waves were presented in the review (Chernov 2006). In application to the ropes of fibers, we associated the periodicity of the latter with the periodic excitation of whistlers attributable to periodic particle injection or bounce period of the particles captured into a small magnetic trap.

The previously published theory (Mann et al. 1989) was based on the threshold switch-on of the loss-cone instability of whistlers when a critical loss-cone angle is exceeded due to an additional perturbation of the magnetic trap (like a FMS wave). However, given the new observational data, this model leaves the various periods of the fibers in ropes, the presence or absence of absorptions, and the fiber frequency splitting without any explanation.

An analogy with the X-ray spikes in tokamak plasmas excited by tearing instability was initially used to explain the rope of fibers on November 3, 1997 (Klassen et al. 2001). In general, however, this process is more suitable for explaining the simultaneous impulsive X-ray bursts and type III bursts.

Subsequently, the same authors suggested a different mechanism, a model with kink instability at anomalous plasma resistance (Karlicky et al. 2002), based on the fact the simplest process can be the density and magnetic field modulation in a loop. It is assumed that the emission should originate from the levels of double plasma resonance, where the upper hybrid frequency ω_{UH} is equal to a whole number (s) of electron cyclotron harmonics $\omega_{Be} : \omega_{UH} = (\omega_{Pe}^2 + \omega_{Be}^2)^{1/2} = s\omega_{Be}$, where ω_{Pe} is the electron plasma frequency (the mechanism by Zheleznyakov and Zlotnik (1975) and Winglee and Dulk (1986) for 3C). The authors describe the electric field of a wave under the action of two oscillators with frequencies ω_{UH} and $s\omega_{Be}$ with a positive feedback. If the local density and magnetic field strength underwent oscillations in time or space, then both these frequencies would undergo the corresponding oscillations. The radio flux, which is proportional to the square of the wave amplitude at the upper hybrid frequency, would then undergo oscillations. Various possible models of these oscillations are considered. In comparison with the wave model (MHD wave) and balloon instability, kink instability at anomalous plasma conductivity was chosen as the most suitable model. The anomalous conductivity is needed to suppress the instability. The effect of rapid heating in a source of small sizes (~10 km) in the shape of a loop with a temperature $T_e \sim 10^7$ K is used.

It is hard to expect the parameters used at the heights of the meter wave band. However, they also allow one to obtain the suppression and recovery of emission (without any overlap in time) with great reserve only for periods of 5–15 s. The short periods of ~1 s cannot be explained, nor can the fiber frequency drift, the formation of absorptions, and other accompanying phenomena (frequency splitting) be explained. Therefore, let us consider in more detail another possible interpretation.

Discussion of the November 3, 1997 Event

According to the IZMIRAN spectra (Fig. 4), even the main rope of fibers at 09:09 UT does not completely satisfy the condition when the succeeding fiber begins only after the switch-off of the emission from the preceding one, although precisely this condition should have justified both the new name and the new mechanism suggested by Klassen et al. (2001) and Karlicky et al. (2002). In addition, the appearance of additional short fibers resembling a frequency splitting at the end of each fiber was disregarded in these papers.

A close relationship is traceable between the appearance of ropes and type III bursts in all four events considered, suggesting a common particle acceleration mechanism. The beams of particles escaping along open field lines produce type III bursts, but some of the particles are trapped. Karlicky et al. (2002) even compare the number of type III bursts with the number of fibers in a rope. In the November 3, 1997 event in the interval 09:08:50–09:09:30 UT, all type III bursts did not drift below approximately 150–160 MHz (Fig. 3), while the presence of many U bursts points to the existence of closed magnetic

loops at these heights in the corona. The formation of ropes exactly near 150 MHz is clearly related to this fact. At this level in the corona, some of the particles were reflected back from the lower CME edge (or the special X point of magnetic reconnection) and conditions for periodic excitation of plasma waves and whistlers were realized in a narrow region of reflection. Thus, our model (Chernov 1997) may also be applicable here if the peculiarities of the conditions in the radio source are taken into account. The narrow band of the fibers (Δf) is related not to the sizes of the trap for particles, but to the narrow range of heights at which the whistlers can propagate until their total cyclotron damping. An even faster termination of emission can be caused by the suppression of plasma wave instability through the interaction of fast particles with whistlers, which deforms the distribution function of the fast particles.

The minimum period of ~1 s in the rope at 210 MHz is precisely determined by the bounce period of the fast particles in the range between 215 MHz ($\sim 0.24 R_\odot$) and 150 MHz ($\sim 0.37 R_\odot$). This range of heights (~90 000 km) are traversed by the fast particles with a velocity of ~1/3 s (typical of type III beams) approximately in 0.9 s. The initial period of ~4.5 s in the main fiber (Fig. 4) is probably related to the capture of particles into a large trap between the shock front located at the height of the plasma level, ~200 MHz ($\sim 0.25 R_\odot$), at 09:09 and the leading CME edge located at a height of $\sim 0.9 R_\odot$ at this time (according to the diagram in Fig. 6). This distance, ~450 000 km, is traversed by the fast particles precisely in 4.5 s. The further increase in period may be related to a new rate of particle acceleration with a gradually increasing period. It should be recognized that each fiber can be associated with a new particle injection, not with the bounce motions of one beam, which is not surprising for such large trap scales, $\sim 0.65 R_\odot$.

In this scheme, the identified ropes of fibers can appear as the whistler wave packets pass through narrow loops with an enhanced density in which the excitation of a small level of plasma waves (flare continuum) is achieved. The periodic whistler packets are most likely generated immediately upstream of the shock front, but they manifest themselves only indirectly, encountering the identified regions with an enhanced level of plasma waves in their path as a result of the coalescence $l + w \rightarrow t$. The reduced frequency drift rate of the fibers in ropes compared to that of ordinary fibers can be explained by the propagation of whistlers inside inhomogeneities (whistler trapping), where their group velocity decreases sharply (Chernov 2007a, 2007b).

It may well be that the enhanced level of plasma waves can be caused by transition radiation; the latter can be responsible for the entire flare continuum emission. The assumption about an important role of transition radiation in the ZP sources was first made by LaBelle et al. (2003).

The appearance of a frequency splitting at the end of fibers is quite admissible in this model. As a result of quasi-linear effects and deformation of the distribution function for fast particles as the maximum in the distribution function shifts to the high velocities, whistlers can be excited along the magnetic field precisely at the end of fibers not only at normal Doppler resonance, but also simultaneously at anomalous one (this effect was considered in detail previously (Chernov 1996)). The emission frequency shifts in accordance with the expression for the cyclotron resonance. The frequency splitting of the ZP stripes estimated previously in terms of this model (Chernov et al. 1998) showed that a splitting of ~2 MHz at 250 MHz required a small shift in the longitudinal particle velocity, from 1.6×10^9 to 2.6×10^9 cm s^{-1}.

CONCLUSIONS

The observational data on four events in combination with previously considered events suggest that the ropes of fibers are usually observed in the time interval when the shock front (even in the absence of the corresponding type II burst) catches up with the leading edge of CME. In large events at the post-maximum flare phase, the ropes can reappear periodically together with new ejections from the flare region accompanied by shock waves near the special X points of magnetic reconnection high in the corona.

Under the condition of a unified approach to interpreting the ropes of fibers in all events, their basic properties can be explained in terms of the standard model of IDBs or fiber bursts by taking into account the plasma parameters in the radio source. The following subtle effects in ropes can be understood by taking into account the behavior of whistlers in the corona and quasi-linear effects when the whistlers are scattered by fast particles: the different periods, durations, and frequency bandwidths of the fibers, the formation of a LF absorption of a different level, and the frequency splitting. The connection of fibers with the developed ZP also becomes clear within the framework of a unified approach to the formation theory of stripes in emission and absorption in the model on whistlers (Chernov 2006).

ACKNOWLEDGMENTS

I wish to thank H. Aurass who provided the spectra of the Tremsdorf station (Astronomical Institute, Potsdam). I am grateful to the SOHO (Solar and Heliospheric Observatory) team for open access to the databases. This work was supported by the Russian Foundation for Basic Research (project no. 05-02-16271).

REFERENCES

1. H. Aurass and G. P. Chernov, Sol. Phys. **84**, 339 (1983).
2. H. Aurass, G. P. Chernov, J. Kurths, et al., Sol. Phys. **108**, 131 (1987).
3. M. Berney and A. O. Benz, Astron. Astrophys. **65**, 369 (1978).
4. G. P. Chernov, Astron. Zh. **53**, 1027 (1976) [Sov. Astron. **20**, 582 (1976)].
5. G. P. Chernov, Astron. Zh. **67**, 126 (1990) [Sov. Astron. **34**, 66 (1990)].
6. G. P. Chernov, Astron. Zh. **73**, 614 (1996) [Astron. Rep. **40**, 561 (1996)].
7. G. P. Chernov, Pis'ma Astron. Zh. **23**, 949 (1997) [Astron. Lett. **23**, 827 (1997)].
8. G. P. Chernov, Astron. Zh. **81**, 938 (2004) [Astron. Rep. **48**, 853 (2004)].
9. G. P. Chernov, Space Sci. Rev. **127**, 195 (2006).
10. G. P. Chernov, A. K. Markeev, M. Poquerusse, et al., Astron. Astrophys. **334**, 314 (1998).
11. G. P. Chernov, M. L. Kaiser, J.-L. Bougeret, et al., Sol. Phys. **241**, 145 (2007a).
12. G. P. Chernov, A. A. Stanislavskii, A. A. Konovalenko, et al., Pis'ma Astron. Zh. **33**, 221 (2007b) [Astron. Lett. **33**, 192 (2007b)].
13. M. Karlicky, M. Barta, A. Klassen, et al., in *Proceedings of the 10th European SPM, "Solar Variability: From Core to Outer Frontiers," Prague, 2002,* ESA SP-506, 1, p. 303.
14. J. I. Khan and H. Aurass, Astron. Astrophys. **383**, 1018 (2002).
15. A. Klassen, H. Aurass, and G. Mann, Astron. Astrophys. **370**, L41 (2001).
16. J. Kuijpers, *Collective Wave-Particle Interaction in Solar Type IV Radio Sources*, Thesis of Utrecht Observ. (Utrech, 1975).
17. A. Kruger, *Introduction to Solar Radio Astronomy and Radio Physics* (Reidel, Dordrecht, 1979; Mir, Moscow, 1984).
18. J. LaBelle, R. A. Treumann, P. H. Yoon, and M. Karlicky, Astrophys. J. **593**, 1195 (2003).
19. O. A. Mal'tseva and G. P. Chernov, Kinem. Fiz. Nebesn. Tel **5**, 44 (1989).
20. G. Mann, K. Baumgaertel, G. P. Chernov, and M. Karlicky, Sol. Phys. **120**, 383 (1989).
21. G. Mann, F. Jansen, R. J. MacDowall, et al., Astron. Astrophys. **348**, 614 (1999).
22. C. Slottje, *Atlas of Fine Structures of Dynamic Spectra of Solar Type IV-dm and Some Type II Radio Bursts* (Utrech Observ., 1981).
23. R. M. Winglee and G. A. Dulk, Astrophys. J. **307**, 808 (1986).
24. V. V. Zheleznyakov and E. Ya. Zlotnik, Sol. Phys. **44**, 461 (1975).

Translated by V. Astakhov